REPORT DOCUMENTATION PAGE

1 AGENCY USE ONLY	2 REPORT DATE 1993	3 TYPE/DATES COVERED
4 TITLE AND SUBTITLE THREE DIMENSIONAL SIMULATION OF STRESS AROUND INCLUSION IN VISCOELASTIC FLUIDS		5 FUNDING NUMBERS
6 AUTHOR B WENDLANDT		
7 FORMING ORG NAMES/ADDRESSES DEFENCE SCIENCE AND TECHNOLOGY ORGANIZATION, MATERIALS RESEARCH LABORATORY, PO BOX 50, ASCOT VALE VICTORIA 3032 AUSTRALIA		8 PERFORMING ORG. REPORT NO
09 SPONSORING/MONITORING AGENCY NAMES AND ADDRESSES		
11SUPPLEMENTARY NOTES		
12 DISTRIBUTION/AVAILABILITY STATEMENT DISTRIBUTION STATEMENT A		12B DISTRIBUTION CODE

13. ABSTRACT (MAX 200 WORDS): A FINITE ELEMENT NUMERICAL MODEL IS PRESENTED WIHICH SIUMLATES VIBRATIONS IN AND AROUND INCLUSIONS IN VISCOELASTIC FLUIDS EXCITED BY A SINUSOIDAL PRESSURE WAVE OR PULSE GENERATED BY NOISY MACHINERY. STRESS TRANSFER PROCESSES ARE INVESTIGATED AND REGIONS OF HIGHEST ENERGY DISSIPATION IDENTIFIED. THE MODEL SIMULATED THE TIME EVOLUTION OF STRESS GENERATION IN AND AROUND INCLUSIONS IN THE VISCOELASTIC PLASTIC FLUID IN THREE SPACE DIMENSIONS FLUID COMPOSITES RECOMMENDED FOR THEIR POWER DISSIPATIVE CHARACTERISTIC ARE RANKED ACCORDING TO THEIR ABILITY TO DISSIPATE ACOUSTIC POWER IN A SIMPLE COMPOSITE STRUCTURE.

14 SUBJECT TERMS			15 NUMBER OF PAGES 15	
			16 PRICE CODE	
17 SECURITY CLASS.REPORT UNCLASSIFIED	18 SEC CLASS PAGE UNCLASSIFIED	19 SEC CLASS ABST. UNCLASS	20 LIMITATION OF ABSTRACT	

Journal of Sound and Vibration (1993) **168**(1), 141–156

2

THREE-DIMENSIONAL SIMULATION OF STRESS AROUND INCLUSIONS IN VISCOELASTIC FLUIDS

B. WENDLANDT

Department of Defence, Materials Research Laboratory, DSTO, P.O. Box 50, Ascot Vale, Victoria 3032, Australia

(*Received 15 November 1989, and in final form 5 June 1992*)

A finite element numerical model is presented which simulates vibrations in and around inclusions in viscoelastic fluids excited by a sinusoidal pressure wave or pulse generated by noisy machinery. Stress transfer processes are investigated and regions of highest energy dissipation identified. The model simulates the time evolution of stress generation in and around inclusions in the viscoelastic plastic fluid in three space dimensions. Fluid composites recommended for their power dissipative characteristics are ranked according to their ability to dissipate acoustic power in a simple composite structure.

1. INTRODUCTION

Many layers of material, which cover engineering structures such as the human body of anechoic and noise and vibration decoupling coatings, are inhomogeneous in structure. The inhomogeneities may be hair roots in skin, or air cavities in anechoic layers, which can maximize dissipation of vibrational or acoustic energy in the layer. The precise manner in which the inhomogeneities, particularly the inserts of air often found in anechoic materials, scatter vibration and acoustic energy is not well understood. Most theoretical approaches which have addressed these problems to date have used fairly simple analytical approaches to describe the mechanisms thought to be involved [1]. The present study aims to complement the analytical work by developing a numerical scheme which may provide a technique for elucidating the areas of uncertainity in the analytical studies of the acoustic response of materials with insets and also media excited by an insert, such as skin pricked by a hair.

A primitive finite difference model is developed which is able to simulate the vibration and acoustic response of a fluid to an incident pressure wave. The fluid may have elastic, viscous and plastic properties and contain inclusions which may be air or fluid.

The fluid is modelled as consisting of a large number of cubical elements which may be distorted by the progression of an acoustic or vibration excitation. The model is able to simulate a limited degree of macroscopic distortion and able to trace the passage of a pressure pulse or sinusoidal wave through a multi-layer, multi-cavity or multi-inclusion fluid, such as coatings used to quieten metal structures or an elastomeric mount designed to attenuate the transmission of sound and vibrations over a wide frequency range, including frequencies at which sections of the mount resonate [2]. The results of representative calculations show the response of cubical cavities and inserts embedded in viscoelastic or plastic media to a sinusoidal excitation. The acoustic response of cylindrical cavities in an elastic fluid is also shown. The model has also been used to simulate the response of surrounds of double cone, diamond and ellipsoidal cavities.

0022-460X/93/250141 + 16 $08.00/0

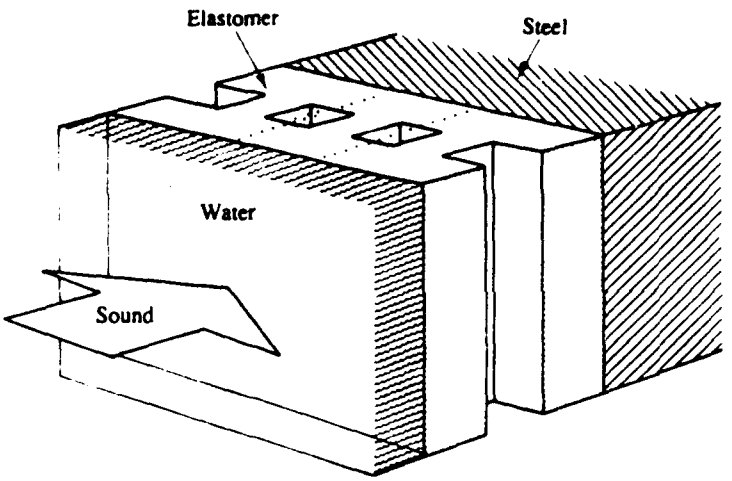

Figure 1. Section of rectangular column cavity modelled and typical surround of cavities. The unit cell is shown by · · ·.

As many fluids used to quieten metal structures are backed by steel plates, the model considers the elastic behaviour of a steel backing plate in calculating the acoustic or vibrational response properties of the fluid systems described. The model permits consideration of water in front of the fluid and air or water behind the steel backing plate.

Typical cross-sections of the fluid coatings which have been modelled are shown in Figure 1 and types of inserts and their pattern in Figure 2. The model is general, however, and is able to represent a wide variety of acoustical and vibrational responses of materials which may be important for anechoic coatings, anti-vibration and acoustic isolation mounts for machinery and the prickle response of the human skin.

2. MODEL

2.1. PROPAGATION MODEL

The propagation of a pressure or stress wave through a compressible medium, such as the fluids considered, is described by the laws of conservation of mass and momentum and the equation of state which relates the pressure or stress in the medium to the strain and its material properties [3].

The displacement of fluid particles by an acoustic wave is small relative to the characteristic dimensions of a typical acoustic structure such as an anechoic coating on a steel plate. The behaviour of such relatively weakly perturbed systems can be solved by numerical methods by using the Lagrangian technique [4]. This technique is particularly suited to calculations in which discontinuities in physical properties, such as density and velocity, occur.

2.2. CONSERVATION OF MASS

The law of conservation of mass for a compressible medium is usually expressed in an Eulerian framework as follows: *the time rate change of mass density at any point is equal to the negative divergence of the momentum at that point*. This law can be expressed in mathematical form in a frame of reference which moves with the fluid, the Lagrangian frame, and is

$$d\rho/dt = -\rho \nabla \cdot \mathbf{v}, \tag{1}$$

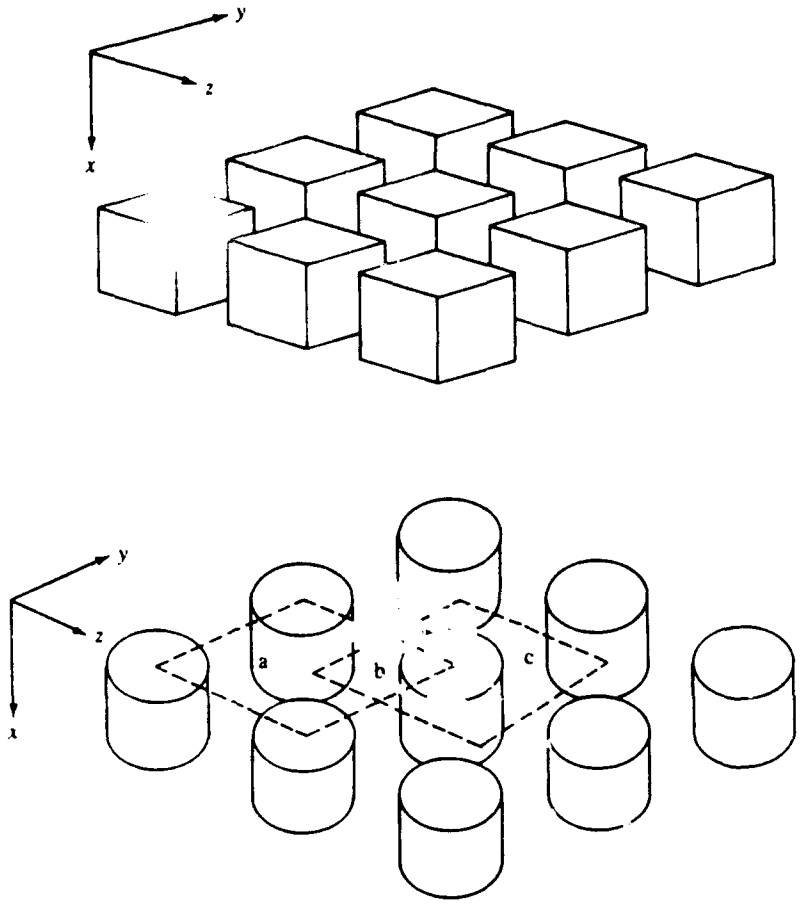

Figure 2. Arrays of typical inserts or cavities. Various unit cells are shown by - - - and labelled a, b and c, respectively.

where ρ is the mass density and $\mathbf{v}$ is the local velocity of the fluid. The discrete numerical representation of the Lagrangian approach defines cells of material corners, and hence boundaries which move with the local fluid velocity. In the present study three-dimensional (x, y, z) space is considered to examine details of shear and normal stresses in the three orthogonal directions. In this system the indices i, j and k indicate cell position counters in the x, y and z directions, respectively. To consider firstly motion in the x direction, the position of a cell corner at time $t + \delta t$, $x_{ijk}(t + \delta t)$ is related to its previous position $x_{ijk}(t)$ at a time t by

$$x_{ijk}(t + \delta t) = x_{ijk}(t) + \int_{t}^{t+\delta t} v_{x_{ijk}}(s)\,\mathrm{d}s. \tag{2}$$

If the velocity variation over the interval δt is represented by an average, the above expression can be written as

$$x_{ijk}^{n+1} = x_{ijk}^{n} + v_{x_{ijk}}^{n+1/2}\,\delta t, \tag{3}$$

where the integer superscript n indicates a particular instant of time via the relationship $t = n\,\delta t$.

Corresponding expressions can be derived for the y and z co-ordinates of the cell corner.

In the time interval $n - 1$ to n, the density variation of the cell designated ijk which is

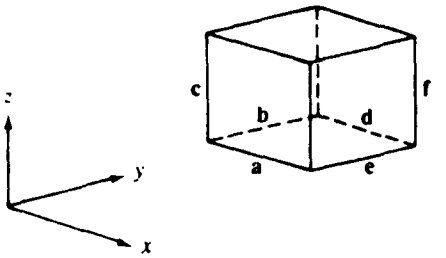

Figure 3. Vectors of element of volume.

bounded by the corner indices ijk, $i+1jk$, $i+1j+1k$, $i+1j+1k+1$, $ij+1k$, $ij+1k+1$, $ijk+1$, $i+1jk+1$, is upon using a vector cross-product notation, given by

$$\rho^n_{ijk} = \rho^{n-1}_{ijk} \frac{\{|\mathbf{c}\cdot(\mathbf{a}\times\mathbf{b})| + |\mathbf{f}\cdot(\mathbf{d}\times\mathbf{e})|\}^{n-1}}{\{|\mathbf{c}\cdot(\mathbf{a}\times\mathbf{b})| + |\mathbf{f}\cdot(\mathbf{d}\times\mathbf{e})|\}^{n}}, \tag{4}$$

where **a**, **b**, **c**, **d**, **e** and **f** are the vectors of the side of the cell shown in Figure 3, and where, for example, **a** is the vector $x, y, z|_{ijk}$ and $x, y, z|_{i+1jk}$.

2.3. CONSERVATION OF MOMENTUM

The law of conservation of momentum is commonly expressed in the moving, Lagrangian frame as

$$\rho \, \mathrm{dv}/\mathrm{d}t = -\nabla p. \tag{5}$$

In a solid material the stress, rather than pressure, causes the cell boundaries to move and rotate [5], and the conservation of momentum is expressed in terms of the stress σ_{ij} and the velocity components along the three axes of Cartesian co-ordinates in tensor notation [6] as

$$\rho \, \mathrm{d}v_i/\mathrm{d}t = \partial\sigma_{ij}/\partial x_j. \tag{6}$$

By extending the one-dimensional situation defined by equation (2) to the three-dimensional case, the velocities of the cell corners are obtained from equation (6), with the discretization of equation (3). These are, for $v_{x_{ijk}}$,

$$v^{n+1/2}_{x_{ijk}} = v^{n-1/2}_{x_{ijk}} + \frac{2\delta t}{\sum_{l=i-1}^{i}\sum_{m=j-1}^{j}\sum_{n=k-1}^{k} \rho^n_{lmn}} \sum_{l=i-1}^{i}\sum_{n=k-1}^{k} \frac{\sigma^n_{xx_{lmn}} - \sigma^n_{xx_{l-1mn}}}{X^n_{lmn} - X^n_{l-1mn}}$$

$$+ \sum_{l=i-1}^{i}\sum_{n=k-1}^{k} \frac{\sigma^n_{xy_{lmn}} - \sigma^n_{xy_{lm-1n}}}{Y^n_{lmn} - Y^n_{lm-1n}} + \sum_{l=i-1}^{i}\sum_{m=j-1}^{j} \frac{\sigma^n_{xz_{lmn}} - \sigma^n_{xz_{lmn-1}}}{Z^n_{lmk} - Z^n_{lmk-1}}, \tag{7}$$

for $v_{y_{ijk}}$,

$$v^{n+1/2}_{y_{ijk}} = v^{n-1/2}_{y_{ijk}} + \frac{2\delta t}{\sum_{l=i-1}^{i}\sum_{m=j-1}^{j}\sum_{n=k-1}^{k} \rho^n_{lmn}} \sum_{l=i-1}^{i}\sum_{n=k-1}^{k} \frac{\sigma^n_{yx_{lmn}} - \sigma^n_{yx_{l-1mn}}}{Y^n_{lmn} - Y^n_{l-1mn}}$$

$$+ \sum_{m=j-1}^{j}\sum_{n=k-1}^{k} \frac{\sigma^n_{yy_{lmn}} - \sigma^n_{yy_{l-1mn}}}{X^n_{lmn} - X^n_{l-1mn}} + \sum_{l=i-1}^{i}\sum_{m=j-1}^{j} \frac{\sigma^n_{yz_{lmn}} - \sigma^n_{yz_{lmn-1}}}{Z^n_{lmk} - Z^n_{lmk-1}}, \tag{8}$$

and for $v_{z_{ijk}}$,

$$v^{n+1/2}_{z_{ijk}} = v^{n-1/2}_{z_{ijk}} + \frac{2\delta t}{\sum_{l=i-1}^{i}\sum_{m=j-1}^{j}\sum_{o=k-1}^{k}\rho^n_{lmo}} \sum_{l=i-1}^{i}\sum_{m=j-1}^{j} \frac{\sigma^n_{zz_{lmk}} - \sigma^n_{zz_{lmk-1}}}{Z^n_{lmk} - Z^n_{lmk-1}}$$

$$+ \sum_{l=i-1}^{i}\sum_{o=k-1}^{k} \frac{\sigma^n_{xy_{ljo}} - \sigma^n_{xy_{lj-1o}}}{Y^n_{ljo} - Y^n_{lj-1o}} + \sum_{m=j-1}^{j}\sum_{o=k-1}^{k} \frac{\sigma^n_{zx_{imo}} - \sigma^n_{zx_{i-1mo}}}{X^n_{imo} - X^n_{i-1mo}}. \tag{9}$$

Here $(X^n_{ijk}, Y^n_{ijk}, Z^n_{ijk})$ is the position vector of the centre of the cell designated ijk at time increment n, the components of which are defined by

$$X^n_{ijk} = \tfrac{1}{8}\sum_{l=i}^{i+1}\sum_{m=j}^{j+1}\sum_{o=k}^{k+1} x^n_{lmo}, \qquad Y^n_{ijk} = \tfrac{1}{8}\sum_{l=i}^{i+1}\sum_{m=j}^{j+1}\sum_{o=k}^{k+1} y^n_{lmo}, \qquad Z^n_{ijk} = \tfrac{1}{8}\sum_{l=i}^{i+1}\sum_{m=j}^{j+1}\sum_{o=k}^{k+1} z^n_{lmo}. \tag{10}$$

This system of equations is complemented by the equation of state of the material, which links the strain experienced by the fluid of the stresses imposed on it, to provide a complete description of the response of a material to an acoustical or vibrational excitation.

2.4. STRAIN-DISPLACEMENT RELATIONS

The strains are determined from the displacement of a particle in a solid or fluid [6]. It is convenient to consider the particle at position x^n_{ijk} at time t of index n to have already received a small displacement $u^n_{x_{ijk}}$ in the x direction so that its undisturbed position was at $x^n_{ijk} - u^n_{x_{ijk}}$. Then, in the present finite primitive element model the displacements along the three axes of the Cartesian co-ordinate system are defined by

$$u^n_{x_{ijk}} = x^n_{ijk} - x^0_{ijk}, \qquad u^n_{y_{ijk}} = y^n_{ijk} - y^0_{ijk}, \qquad u^n_{z_{ijk}} = z^n_{ijk} - z^0_{ijk}. \tag{11}$$

The incremental change of these displacements leads to the deformation of an element of volume and can be expressed mathematically in terms of the divergence and curl [10] of the displacement. For instance, the deformation of the element of volume in the x direction can be expressed, by the chain rule [6, 7], as

$$\delta u^n_{x_{ijk}} = \frac{\partial u^n_{x_{ijk}}}{\partial x}\delta x_{ijk} + \tfrac{1}{2}\left(\frac{\partial u^n_{x_{ijk}}}{\partial y} + \frac{\partial u^n_{y_{ijk}}}{\partial x}\right)\delta y_{ijk} - \tfrac{1}{2}\left(\frac{\partial u^n_{y_{ijk}}}{\partial x} - \frac{\partial u^n_{x_{ijk}}}{\partial y}\right)\delta y_{ijk}$$

$$+ \tfrac{1}{2}\left(\frac{\partial u^n_{x_{ijk}}}{\partial z} + \frac{\partial u^n_{z_{ijk}}}{\partial x}\right)\delta z_{ijk} - \tfrac{1}{2}\left(\frac{\partial u^n_{z_{ijk}}}{\partial x} - \frac{\partial u^n_{x_{ijk}}}{\partial z}\right)\delta z_{ijk}. \tag{12}$$

This may be expressed in mathematical shorthand by

$$\delta u^n_{x_{ijk}} = \epsilon^n_{xx_{ijk}}\delta x_{ijk} + \epsilon^n_{xy_{ijk}}\delta y_{ijk} - \epsilon^n_{xy_{ijk}}\delta y_{ijk} + \epsilon^n_{xz_{ijk}}\delta z_{ijk} - \epsilon^n_{xz_{ijk}}\delta z_{ijk}, \tag{13}$$

where higher order terms in δx^n_{ijk}, δy^n_{ijk} and δz^n_{ijk} have been neglected. The $\epsilon^n_{xy_{ijk}}$ and $\epsilon^n_{xz_{ijk}}$ represent rotation. The $\epsilon^n_{xx_{ijk}}$, $\epsilon^n_{xy_{ijk}}$ and $\epsilon^n_{xz_{ijk}}$ represent the direct and symmetric strains needed to compute the stresses induced in the material. The strains at the cell centres of the number scheme used here are related to the displacements at the cell corners by

$$\epsilon^n_{xx_{ijk}} = \tfrac{1}{4}\sum_{m=j}^{j+1}\sum_{o=k}^{k+1} \frac{u^n_{x_{i+1mo}} - u^n_{x_{imo}}}{x^n_{i+1mo} - x^n_{imo}}, \qquad \epsilon^n_{yy_{ijk}} = \tfrac{1}{4}\sum_{l=i}^{i+1}\sum_{o=k}^{k+1} \frac{u^n_{y_{lj+1o}} - u^n_{y_{ljo}}}{x^n_{lj+1o} - x^n_{ljo}},$$

$$\epsilon^n_{zz_{ijk}} = \tfrac{1}{4}\sum_{m=i}^{i+1}\sum_{l=i}^{i+1} \frac{u^n_{z_{lmk+1}} - u^n_{z_{lmk}}}{z^n_{lmk+1} - z^n_{lmk}}, \tag{14–16}$$

and

$$\epsilon^n_{xx_{ijk}} = \frac{1}{8}\left(\sum_{m=j}^{j+1}\sum_{o=k}^{k+1}\frac{u^n_{x_{i+1mo}} - u^n_{x_{imo}}}{x^n_{i+1mo} - x^n_{imo}} + \sum_{l=i}^{i+1}\sum_{o=k}^{k+1}\frac{u^n_{y_{lj+1o}} - u^n_{y_{ljo}}}{y^n_{lj+1o} - y^n_{ljo}}\right). \tag{17}$$

$$\epsilon^n_{xz_{ijk}} = \frac{1}{8}\left(\sum_{m=j}^{j+1}\sum_{o=k}^{k+1}\frac{u^n_{z_{i+1mo}} - u^n_{z_{imo}}}{x^n_{i+1mo} - x^n_{imo}} + \sum_{l=i}^{i+1}\sum_{m=j}^{j+1}\frac{u^n_{x_{imk+1}} - u^n_{x_{imk}}}{z^n_{imk+1} - z^n_{imk}}\right). \tag{18}$$

$$\epsilon^n_{zy_{ijk}} = \frac{1}{8}\left(\sum_{l=i}^{i+1}\sum_{o=k}^{k+1}\frac{u^n_{z_{lj+1o}} - u^n_{z_{ljo}}}{y^n_{lj+1o} - y^n_{ljo}} + \sum_{l=i}^{i+1}\sum_{m=j}^{j+1}\frac{u^n_{y_{imk+1}} - u^n_{y_{imk}}}{z^n_{imk+1} - z^n_{imk}}\right). \tag{19}$$

The displacements at cell corners are calculated by integrating the velocities at the corners via equation (3).

2.5. STRESS–STRAIN RELATIONS AS EQUATIONS OF STATE

The simple theory of elasticity assumes that the induced stresses and strains are linearly related to each other and that the stress and strain tensors always have the same axes. If the stresses and strains along three orthogonal axes are considered, then the general stress–strain relation can be written as [6],

$$\sigma_{ij} = \lambda\epsilon_{mm}\delta_{ij} + 2\mu\epsilon_{ij}. \tag{20}$$

The parameter $\epsilon_{mm}\delta_{ij}$ represents the sum of the orthogonal strains; λ and μ are known as Lamé's constants and μ is also called the modulus of rigidity and measures the resistance of the substance to distortions. These constants are related to Young's modulus E and the Poisson ratio ν by

$$\lambda = \nu E/(1+\nu)(1-2\nu), \qquad \mu = E/2(1+\nu). \tag{21, 22}$$

The stress situation is described as hydrostatic when the direct stresses in three orthogonal directions are equal and the shear stresses are zero. The direct strains will then be equal. Under these conditions, in general

$$\sigma_{xx} = \sigma_{zz} = 3k\epsilon_{xx} = 3k\epsilon_{zz} \tag{23}$$

where $k = \lambda + 2\mu/3$. The parameter k is called the bulk modulus because the relative change of volume if $3\epsilon_{xx}$ to first order, so that k is the ratio of the symmetrical stress to the change in volume. For an ideal fluid, $\mu = 0$ and $k = \lambda$.

In materials which behave in a hysteretic, lossy fashion a phase delay is induced in acoustic signals propagating through them. Accordingly such materials are characterized by Lamé constants involving differential operators with respect to time in the time domain and complex constants in the frequency domain [1].

Equation (20) decomposes in the orthogonal co-ordinate (x, y, z) system used in the present simulation model at any instant of time defined by the time index n to

$$\sigma^n_{xx} = (\lambda + 2\mu)\epsilon^n_{xx} + \lambda(\epsilon^n_{yy} + \epsilon^n_{zz}) \tag{24}$$

and

$$\sigma^n_{yy} = (\lambda + 2\mu)\epsilon^n_{yy} + \lambda(\epsilon^n_{xx} + \epsilon^n_{zz}), \qquad \sigma^n_{zz} = (\lambda + 2\mu)\epsilon^n_{zz} + \lambda(\epsilon^n_{xx} + \epsilon^n_{yy}). \tag{25, 26}$$

Also, $\sigma^n_{xy} = \sigma^n_{yx} = 2\mu\epsilon^n_{xy}$, $\sigma^n_{zx} = \sigma^n_{xz} = 2\mu\epsilon^n_{xz}$ and $\sigma^n_{zy} = \sigma^n_{yz} = 2\mu\epsilon^n_{yz}$, where λ and μ involve differential operators with respect to time for lossy materials.

2.6. STRESS–STRAIN RELATIONS FOR LINEAR PLASTIC – VISCOELASTIC MATERIALS

The vibrational behaviour of many fluids, or materials which behave like fluids such as elastomers, varies with temperature, pressure and rate of strain. The elastic behaviour may vary when stresses are repeatedly reversed and the material may exhibit hysteresis. Once the yield point of a substance exhibiting plastic behaviour is passed, increasing stresses give steadily increasing strains. Hence any single mathematical model can be expected only to approximate the elastic behaviour of actual substances under limited conditions [5]. The behaviour of all the fluids considered in this study is, to a good approximation, linear for the small pressure fluctuations considered to be typical of acoustic and vibration generated by machinery.

The simplest general linear relationship between a change in stress and associated strain can be written in tensor notation as

$$\sigma_{ij} + t_0 \partial\sigma_{ij}/\partial t = \lambda(1 + t_1 \partial/\partial t)\varepsilon_{mm}\delta_{ij} + 2\mu(1 + t_2 \partial/\partial t)\varepsilon_{ij}. \tag{27}$$

where t_0, t_1 and t_2 are characteristic relaxation times of the material.

Plastic behaviour is described by the condition that, for a constant stress σ_{ij} applied at $t = 0$, the material response can be characterized as follows [8]:

$$\sigma_{ij} + (\sigma_i - \sigma_0)t/t_3 = \lambda(1 + t_1 \partial/\partial t)\varepsilon_{mm}\delta_{ij} + 2\mu(1 + t_2 \partial/\partial t)\varepsilon_{ij} \qquad \text{if } \sigma_{ij} \geq \sigma_0. \tag{28}$$

The t_3, t_2 and t_1 are characteristic relaxation times of the material, and describe the complex nature of the elastic moduli in the time domain used commonly in steady state impedance fomulations.

The linear model of equations (27) and (28) gives a representation of damping of vibrations by internal friction. The internal friction causes a phase delay in the transmission of steady sinusoidal signals through the material which can be expressed as a loss-tangent, $\tan\delta$, which is related to the relaxation times and the frequency ω of the signal by

$$\tan\delta_\lambda = \omega(t_1 - t_0)/(1 + \omega^2 t_1 t_0), \qquad \tan\delta_\mu = \omega(t_2 - t_0)/(1 + \omega^2 t_2 t_0). \tag{29, 30}$$

The angle δ measures the lag of strain behind stress, and is known as the loss angle of the material and provides a measure of the internal damping of stress waves [5].

The loss tangents of materials commonly used in acoustic structures cannot always be related to the excitation frequency as described by equations (29) and (30). The magnitudes of t_0, t_1 and t_2 vary with frequency such that a simpler Kelvin–Voigt model [5], where $t_0 = 0$, might be adequate to describe the anechoic coating under consideration. The more general formalism of equations (27) and (28) is kept to widen the range of acoustic structures which can be studied by the present model. In particular, many elastomers are characterized by different values for the loss tangent associated with the first and second Lamé constants which is reflected in the time differential operator coefficients of these constants in equations (27) and (28).

The viscoelastic stress–strain equation can be expressed in a finite cell formulation which relates the stress tensor σ_{ij} at time index n and cell centre (ijk) to the corresponding strain tensor arising from the movement of the adjoining cell corners (see Figure 4) by using backward differences for the time step, where the ε's are calculated from the movement at cell corners. The numerical procedure for evaluating velocity and displacement at the cell corners and density and stresses and strain at cell centres enhances the computational stability of the Lagrangian technique used.

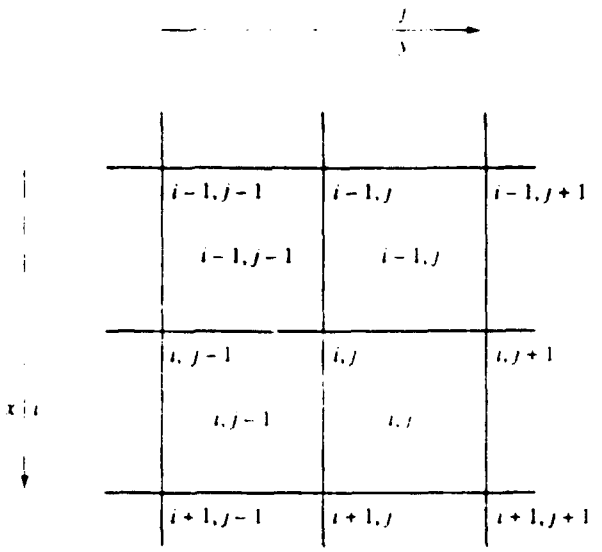

Figure 4. The two-dimensional (x, z) section of the three-dimensional space grid used to circumscribe cells and define cell centres

2.7. LOSS FUNCTION

Power dissipation considered is caused by loss mechanisms which become active during the deformation of the material. The power dissipated by these mechanisms is given by dW/dt, where W is the work done by the stresses across the surface of an element of volume $\delta\tau = \delta x\,\delta y\,\delta z$, and the forces $\rho\,\delta v_x\,\delta t$, $\rho\,\delta v_y\,\delta t$ and $\rho\,\delta v_z\,\delta t$.

For an infinitesimal increment of displacement the work increment per unit volume is given, in tensor notation for simplicity [3], by

$$\delta W' = \sigma_{ij}\,\delta\epsilon_{ij}, \tag{31}$$

where the summation signs may be omitted under the summation convention for tensors [9]. The work increment $\delta W'$ and the time increment δt can be related by

$$\delta W'/\delta t = \sigma_{ij}\,\delta\epsilon_{ij}/\delta t, \tag{32}$$

where the instantaneous power absorbed is given by dW'/dt as δt approaches zero.

If the incident wave is steady state cyclic with angular frequency ω, the average power dissipated per unit volume is of interest. This can be written as

$$L = \frac{\omega}{2\pi\delta\tau}\int_{t}^{t+2\pi/\omega}\frac{dW'}{dt}\,dt. \tag{33}$$

Taking limits in equations (32) and substituting in equation (33) gives

$$L = \frac{\omega}{2\pi}\int_{t}^{t+2\pi/\omega}\sigma_{ij}\frac{d\epsilon_{ij}}{dt}\,dt. \tag{34}$$

where t is the time at the beginning of the cycle, $t + 2\pi/\omega$ is the time at the end of the cycle and $2\pi/\omega$ is the period of the cycle. In the numerical scheme used in the present work, this loss function L at all cell locations ijk is calculated from

$$L_{ijk} = \frac{\omega}{2\pi}\sum_{n=t/\delta t}^{n=(t+2\pi/\omega)/\delta t}\sigma^{n}_{ijk}\,(\epsilon^{n}_{ijk} - \epsilon^{n-1}_{ijk}). \tag{35}$$

The units of L is watt per cubic metre (W m^{-3}).

3. CALCULATIONS

The model was programmed to simulate the acoustic and vibrational response of fluid layers containing several types of cavities or inserts to investigate the effect the cavity or insert shape has on the global acoustic properties of such layers. The main shapes of cavities or inserts investigated were columns, cubes and short cylinders.

The cavities or inserts were considered to be spaced at regular intervals which permits the consideration of a unit cell only. Typical unit cells containing a portion or all of a cavity or insert are shown in Figures 1 and 2 by dashes. The cavities or inserts were 5 mm in diameter or square and spaced 5 mm apart. The acoustic structure was assumed to be made up of a layer of such unit cells extending to infinity in the y and z direction. Each unit cell was assumed to behave in an identical manner with continuity of excitation across unit cell interfaces.

The calculations were carried out in the order shown in the flowchart of Figure 5. A sinusoidal excitation in the x component of the velocity vector was started at plane $i = 1$ at time $t = 0$ or time increment $n = 0$. The displacements of the cell corners were calculated from equation (3) using equations (7)–(9). A cross-section of the primitive finite element grid used in the present model is shown in Figure 4. The volumes of the cells and local density of material was updated. Finally, the stresses were updated to complete one cycle

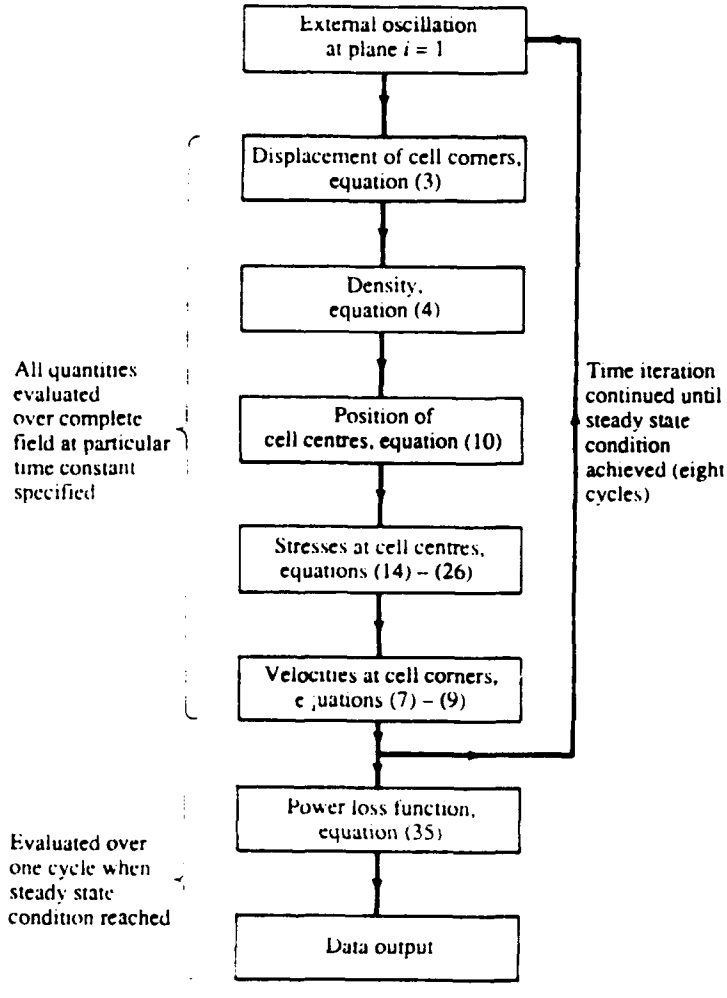

Figure 5. Flowchart of computation

of iteration. The acoustic structures considered required about five cycles of excitation before steady state vibrational responses were observed. Computer memory and computing time considerations limited the number of cells in the calculations to 60 along each axis of the Cartesian co-ordinate system.

Simulations were first carried out for both loss-less and lossy elastomer half-spaces containing no cavities or inserts to check the accuracy of the computations against analytical results. The tests indicated that the amplitudes of displacements computed were accurate to within half of one percent. Calculations were then carried out to check the extent to which the computations conserved energy in the system modelled. The calculations were estimated to conserve energy to about 95 percent. This figure was considered good for the spatial grid used and the complexity of the calculations involved [10]. It was estimated that the numerical calculations conserved energy or power to about 90 percent for the system modelled.

4. RESULTS

The acoustic behaviour of sound-absorbing or dissipative structures can conveniently be described in terms of the behaviour of regions where the major responses to the acoustic excitation occur. These regions can be considered to be elements of the overall acoustic structure [1].

The details of the vibrational and acoustic response of material around and in inclusions is most readily presented by considering first the two space dimensional response of columnar inserts in a medium, such as the rectangular columns shown in Figure 1 and similar cylindrical columns, where the vibrational excitation is perpendicular or normal to the long axis of the column.

The acoustic response of the background medium is most clearly presented by considering first the case in which the speed of sound in the insert is very small compared with the speed of sound in the background medium. Such a composite scatters the sound at the acoustically soft surface of the insert and facilitates its absorption though mode conversion, where the shear modulus of the medium enhances the absorption of the acoustic excitation. The insert material with the lowest practical speed of sound is air, and hence the stresses generated around air inserts or cavities embedded in a viscoelastic medium will be presented first. When a dilatational wave encounters such cavities, the wave is reflected by the acoustically soft boundary at the cavity surface [11] and some transformation of normal stress into transverse and shear stress occurs.

4.1. INTER-INSERT REGION AND INSERT EDGES

4.1.1. *Inter-insert column*

The generation of shear stress is widely considered to be an indication of acoustic absorption efficiency [12] and hence computational simulations of shear around inserts in viscoelastic layers are shown in Figures 6–12. The acoustic response of a column of rectangular cross-section is illustrated by patterns of shear stresses shown in Figure 6. The coating material is forced into each cavity by the transformation of normal into shear stress through Poisson's effect. This causes the pattern of shear stress in the inter-cavity region to have a node along the centre of the column. Symmetry and conservation of angular momentum require that edges on opposite sides of the material column between the cavities rotate in opposite directions. The stresses are concentrated at the corners of the cavities facing the acoustic excitations in the examples shown because mode relaxation removes energy from the incident excitation before it reaches the corners further away; and

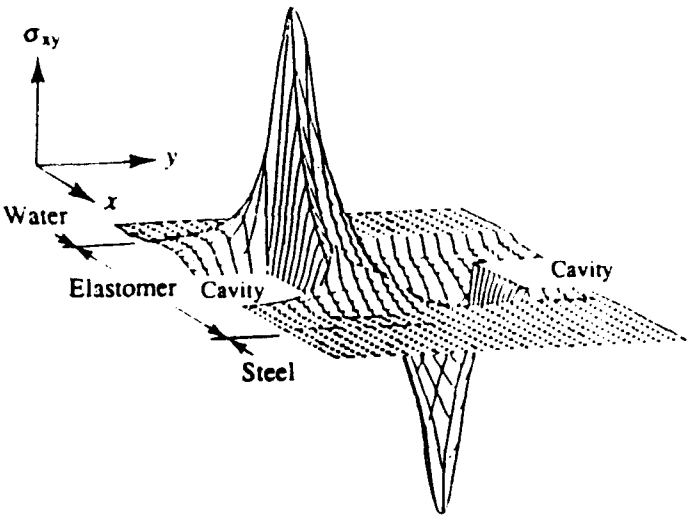

Figure 6. Shear stress around cavity edges of columnar cavity showing phasing relationship. Excitation incident from top, water-side of figure along x-axis.

viscoelastic losses in the material in these examples (see Table 1) have also caused attenuation of the acoustic wave during its transit.

4.1.2. *Cubical inserts*

The acoustical response of a cubical insert or cavity (see Figure 2), is similar to that of a rectangular column. The edges facing the incident acoustic excitation are centres of shear, σ_{xy}; see Figure 7. The major difference occurs in the σ_{yy}, which is of course 0 for a column.

TABLE 1

Material parameters: bromobutyl rubber and surrounds

Elastomer			Steel			Water
Young's modulus, E (Pa)	Poisson ratio, ν	Density, ρ (kg/m^3)	Young's modulus E (Pa)	Poisson ratio, ν	Density ρ (kg/m^3)	Density ρ (kg/m^3)
$5{\cdot}0 \times 10^6$	0·49	1130	$1{\cdot}6 \times 10^{10}$	0·26	7800	1000

Elastomer			
Frequency, ω (kHz)	Loss tangent, $\tan \delta_L$	Relaxation time constants t_1, t_2 (s $\times 10^{-4}$)	t_0 (s $\times 10^{-5}$)
10	0·612	2·1	6·5
16	0·634	1·3	4·5
25	0·650	0·88	2·6
40	0·669	0·56	1·6
65	0·684	0·36	0·99
100	0·695	0·24	0·65

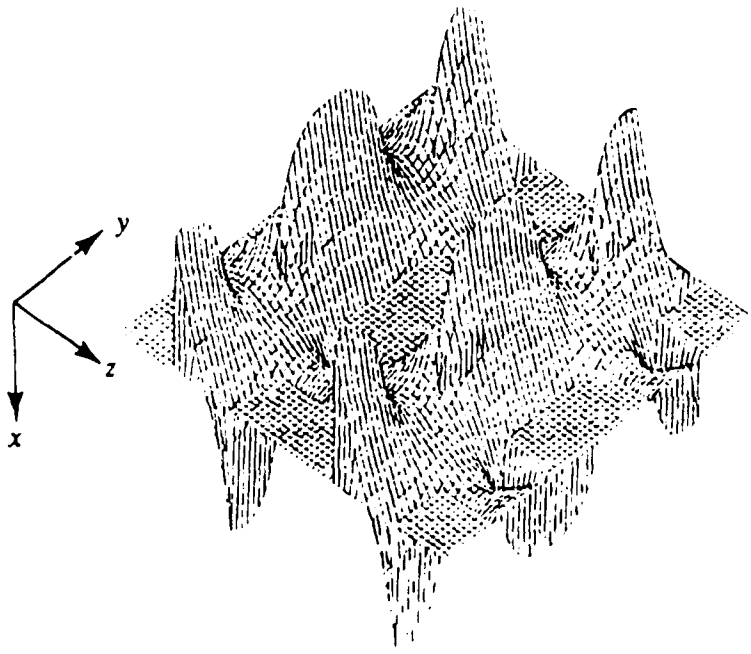

Figure 7. Shear stress σ_{xz} rotating about the y-axis around cubical cavities, showing the phasing relationship around and between cavities. Excitation from above figure in direction of x-axis.

and which for square cavities has maxima at the edges in line with the direction of advance of the incident acoustic wave. The shear rotating about the x-axis, σ_{yz}, is shown in Figure 8.

4.1.3. *Cylindrial inserts*

The response of a cylindrical cavity excited normal to its long axis is similar to that of a rectangular column. The shear stress pattern is shown in Figure 9.

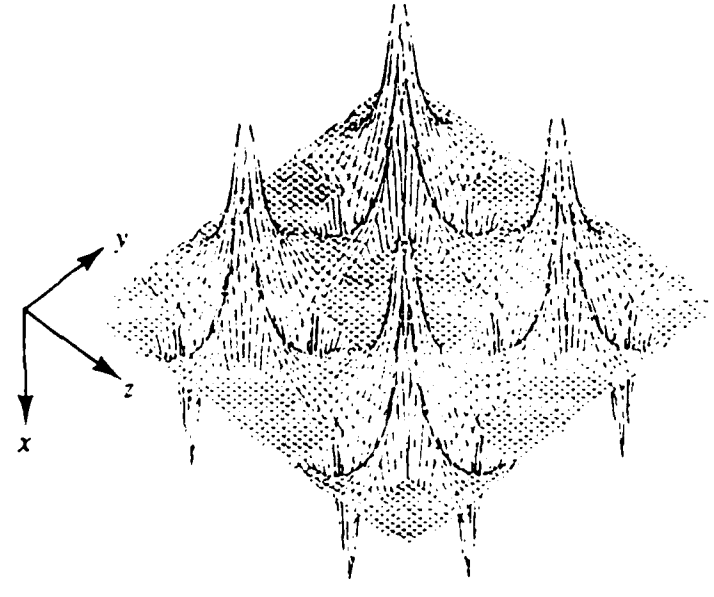

Figure 8. Shear stress σ_{yz} rotating about the x-axis around cubical cavities, showing the phasing relationship around and between cavities. Nodal lines are readily visible. Excitation from above figure in direction of x-axis.

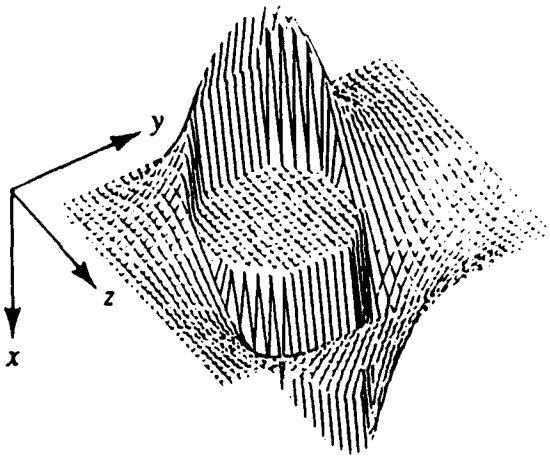

Figure 9. Shear stress σ_{xy} rotating about the z-axis around cylindrical column cavities, showing phasing relationship. Excitation from direction of y-axis.

When a cylindrical air-filled cavity is acoustically excited along its long axis, the response of the surrounds is similar to that of a square column for the σ_{xy} and σ_{xz} stress as expected; see Figure 10. The σ_{xy} rotates about the z-axis and the σ_{xz} rotates about the y-axis. Additional motion occurs around the circumference of the cylinder. The associated shear stress rotating about the x-axis is shown in Figure 11. Conservation of momentum requirements require that the basic response is a two-wavelength shear strain excitation. The presence of neighbouring cavities is believed to limit the cylinder response to this basic mode. This result is of importance in designing resonance absorption into acoustic energy absorbing structures.

4.1.4. *Diamond and double pyramid cavities*

The transformation of normal into shear stress is enhanced at the point of these cavities where the spatial gradient of the material properties are greater than for the cavities

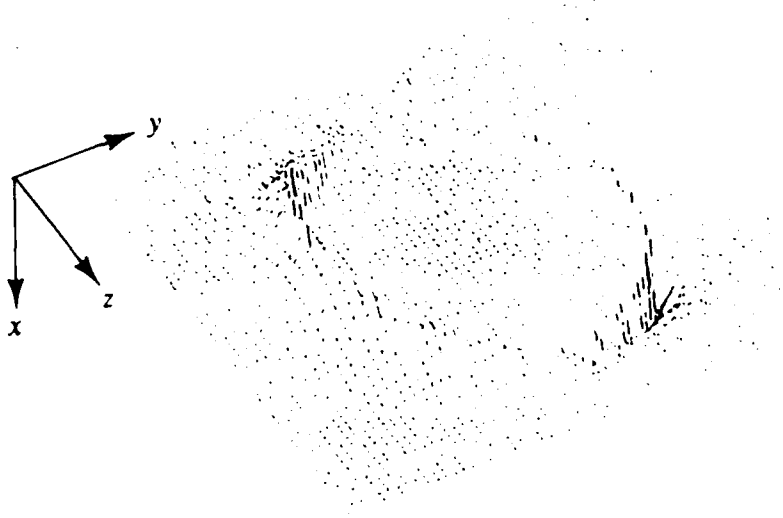

Figure 10. Shear stress σ_{xy} rotating about the z-axis around the upper rim of a cylindrical cavity, showing the phasing relationship. Excitation from above figure in direction of x-axis.

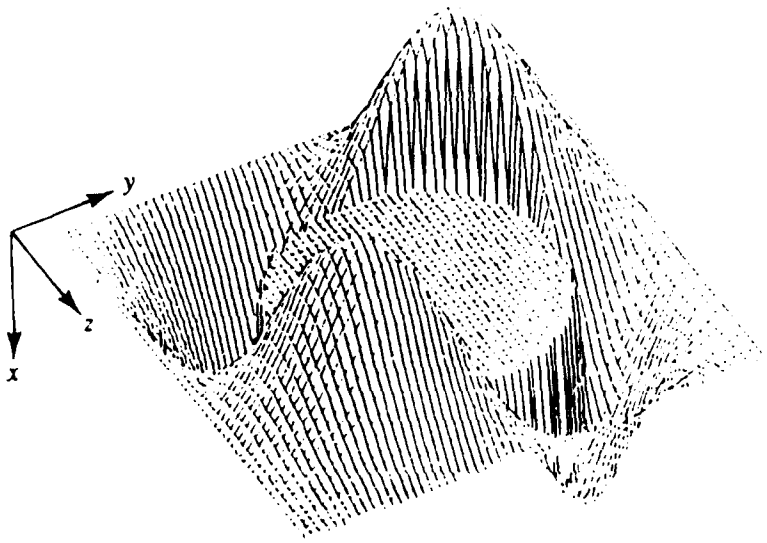

Figure 11. Shear stress σ_{xy} rotating about the x-axis around a cylindrical cavity, showing phasing relationship. The excitation was incident from above figure along direction of x-axis.

considered so far. A typical shear stress pattern around the point is similar to that observed at a corner in square cavities and around cylindrical cavities.

4.1.5. *Solid inserts*

Typical shear stresses in and around solid, square, column inserts the acoustic impedance, but not the speed of sound, of which is equal to that of the background matrix material, are shown in Figure 12. The shear stress is zero at the surface in accordance with acoustic theory and concentrated along the material interfaces where the sound waves in

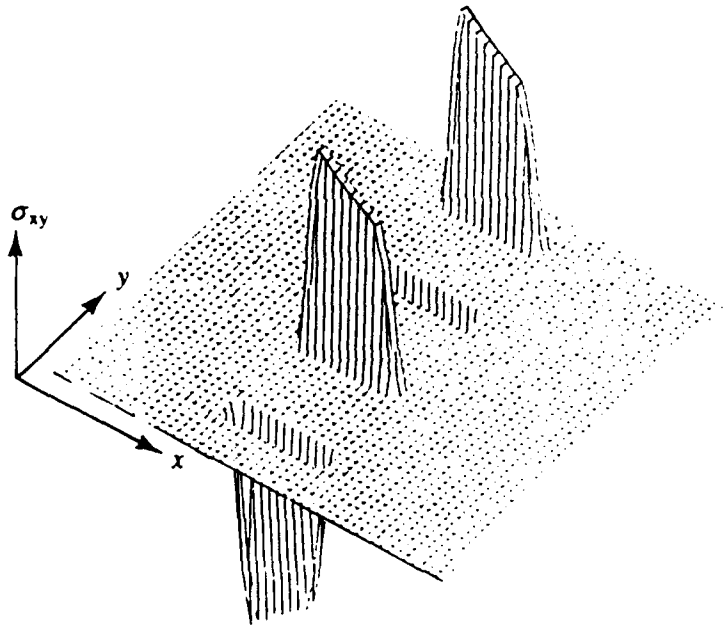

Figure 12. Shear stress σ_{xy} rotating about the z-axis around an insert the acoustic impedance, but not the speed, of which is equal to that of the background matrix material. Excitation was along the x-axis.

the two media are out of phase. Similar patterns of stress were computed for cubical inserts such as shown in Figure 2.

5. ENERGY DISSIPATION

Energy dissipation properties determined the efficiency with which an element of a given material composite attenuates sound and vibration and is fundamental for the design of sound-attenuating coatings and machinery mounts. Irreversible energy losses in hysteretic fluids, such as viscoelastic elastomers or plastic materials are caused by particle–particle interaction when an element of the fluid is distorted by the acoustic or vibrational stress wave. These losses are proportional to the product of time rate of change of strain and stress, denoted by L in equation (33), and hence are dominant at the corners of cavities and edges of inserts where both strain and stress change rapidly. This general picture of the energy dissipation in the material changes only slightly with frequency.

TABLE 2

Relative power dissipation in composites

Thickness of composite = 0·5 cm coating; insert shape is rectangular columns; insert size = 0·5 cm wide, spaced 0·5 cm apart; facing material is water; backing material is steel; frequency of acoustic excitation = 100 kHz; number of computed oscillations = 3

		Material properties									
		Background					Insert				
Composites	Power loss, L_r	λ	tan δ_λ	μ	tan δ_μ	ρ	λ	tan δ_λ	μ	tan δ_μ	ρ
A	0·30	0·854	0·000	0·689	0·010	0·689	0·606	0·0	0·000	0·16	2·0
B	0·00	0·531	0·0	0·000	0·12	1·02	0·527	0·0	0·004	0·09	1·7
C	0·01	0·854	0·0	0·689	0·01	1·689	1·334	0·0	0·444	0·50	4·0
D	2·6	0·854	0·0	0·689	0·01	1·689	0·150	0·0	0·000	0·16	2·0
E	0·01	0·444	0·0	0·000	0·0	1·0	1·334	0·0	0·444	0·50	4·0
F	0·00	0·444	0·0	0·000	1·0	1·0	1·334	0·0	0·444	0·50	1·0
G	1·00	0·824	0·001	0·209	0·01	1·213	0·604	0·0	0·000	0·16	2·0
H	23·00	0·419	0·002	0·209	0·01	1·99	0·159	0·0	0·000	0·16	4·0

Here λ and μ are the first and second Lamé constants of the material; tan δ_λ and tan δ_μ are the associated loss-tangents, and ρ denotes the density of the respective material. The material properties are normalized with respect to the density and equivalent material modulus of water ($c^2\rho$, where c is the speed of sound in water), and the power loss is normalized with respect to that of material combination G. Thus all parameters in this table are dimensionless.

	Material	
Composite	Background	Insert
A	syntactic foam	heavy silicone rubber
B	silicone rubber	heavy silicone rubber
C	syntactic foam	heavy loaded plastic
D	syntactic foam	heavy loaded silicone foam
E	silicone rubber	heavy loaded plastic
F	silicone rubber	plastic
G	plastic	heavy silicone rubber
H	heavy plastic	heavy loaded silicone rubber

5.1. RANKING OF ACOUSTIC POWER DISSIPATING COMPOSITES

Researchers in the acoustic attenuation field have surveyed the range of practical, energy dissipative composites [1] which are suitable for noise absorbing structures. The composites examined are shown in Table 2. The composites consist of elastomer inserts in a plastic-like background material. To illustrate the usefulness of the present model, it was used rank the average power dissipation properties of the composites shown in Table 2 for simple square columns. The relative average power dissipated by the various composites is denoted by L, and is shown in Table 2 [1]. The average power dissipation L, is normalized to the loss of a composition believed to be a practical composite. The calculations underlaying this ranking did not consider resonance effects due to size or shape.

ACKNOWLEDGMENT

Mr Allen Jenkins deserves praise for running, maintaining and writing computer codes required for the production of many of the results and figures.

REFERENCES

1. K. P. SCHARNHORST, W. M. MADIGOSKY and E. BALIZER 1985 *Report NSWC TR* 85-196 Scattering coefficients and the absorption edge of longitudinal coherent sound waves in selected inhomogeneous materials.
2. J. C. SNOWDON 1968 *Vibration and Shock in Damped Mechanical Systems*. New York: John Wiley.
3. A. SOMMERFELD 1964 *Mechanics of Deformable Bodies*. New York: Academic Press.
4. D. P. POTTER 1973 *Computational Physics*. New York: John Wiley.
5. J. C. JAEGER 1956 *Elasticity, Fracture and Flow*. London: Methuen.
6. H. JEFFREYS and B. S. JEFFREYS 1962 *Mathematical Physics*. Cambridge: University Press.
7. F. B. HILDEBRAND 1962 *Advanced Calculus for Applications*. New York: Prentice-Hall.
8. J. C. JAEGER 1981 *An Introduction to Applied Mathematics*. Oxford: Clarendon Press.
9. M. F. SPIEGEL 1959 *Vector Analysis*. New York: Schaum.
10. D. L. BROWN 1984 *Mathematics of Computation* **42**(166), 369–391. A note on the numerical solution of the wave equation with piecewise smooth coefficients.
11. H. KOLSKY 1953 *Stress Waves in Solids*. Oxford: Clarendon Press.
12. W. MADIGOSKY 1988 Personal communications.